Boundary Layer Assessment of INTONATE Model

Haley Naik[1], Meike Jansen[2], Michael Mößner[3], Nan Hu[4]

Institute of Aerodynamics and Flow Technology, German Aerospace Center (DLR)

E-Mail: [1] haley.naik@dlr.de, [2] meike.jansen@dlr.de, [3] michael.moessner@dlr.de, [4] nan.hu@dlr.de

Introduction

During the wind tunnel tests of the DLR INTONATE project on a model of a short- and medium-range aircraft, a detailed investigation of the boundary layer development was carried out on the model-cockpit. For this study a boundary layer rake, with 29.6mm height mounted over various cockpit positions, was used to determine boundary layer thicknesses (δ) and boundary layer edge velocities (U_e). The test results were then validated using three CFD simulations with different numerical methods. The course of the boundary layer for most of the measured positions seems to be identical to that of the simulations.

Motivation

Wall pressure fluctuations within a turbulent boundary layer (TBL) causes vibration of the structure which in turn leads to aircraft cabin noise. This prolong exposure to noise during the entire flight causes passenger discomfort. Therefore, the prediction of the wall pressure fluctuations becomes an important research topic. Over time many empirical models have been developed to predict wall pressure fluctuations. Goody [1] developed an empirical model for two-dimensional zero pressure gradient (ZPG) boundary layer, whereas Rozenberg et al. [2] proposed the model for adverse pressure gradient (APG) flows. Hu and Herr [3], considered the pressure fluctuations on a flat plate for both adverse and favourable pressure gradient (FPG) boundary layer. These models, thus developed, use boundary layer characteristics as well as the effects of pressure gradients to evaluate wall pressure fluctuations and their characteristics. The objective behind the current measurements was to implement empirical wall pressure spectra model and analyse the flow around the aircraft cockpit.

Experimental Setup

Wind tunnel tests for the present study were conducted on a quarter scale aircraft cockpit model in the closed test-section of DNW-NWB. This cockpit model was instrumented with 22 Kulite Sensors on one half [4] and MEMS sensor arrays on the other half. A similar concept was presented by Salze et al. [5], where he measured boundary layer profiles using hot-wires on a realistic full-scale business jet cockpit model. In the present test, a boundary layer rake of total height of 29.6mm measuring total pressure by means of 37 pressure probes was installed on 8 positions as shown in Fig. 1:

- **One** on the cockpit windshield,
- **Two** on the top and
- **Five** side of the cockpit

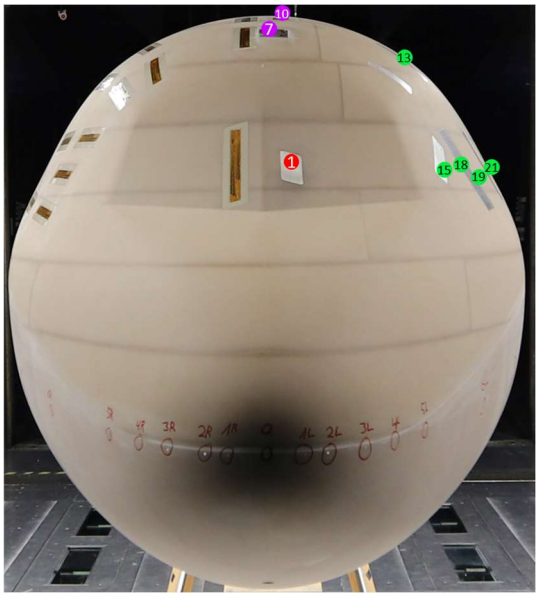

Figure 1: Boundary layer rake mounted on the side of the cockpit

The first probe is approximately at a distance of 0.48mm above the model's surface as shown in Fig. 2. The experimental data was evaluated for the free flow velocities (U_∞) ranging from 30-60m/s and angles of attack (α) from -1° to 6°. The present study targets the reference flow conditions only as defined to a velocity of 50m/s and 3° angle of attack.

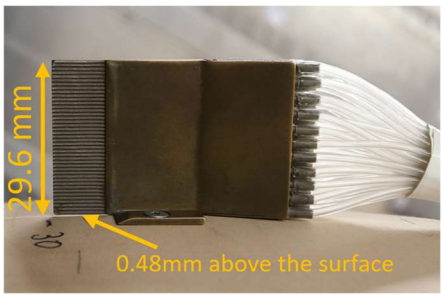

Figure 2: Rake specifications

Simulation Strategy

To validate the experimental results, an extensive comparison of wall resolved RANS (Reynolds-averaged Navier-Stokes) simulations was performed using DLR-TAU Code and simulated on DLR HPC-Cluster CARA. This includes:

- $k-\omega$ Menter SST turbulence model with **Farfield**
- Reynolds Stress model with **Farfield**
- Spallart-Allmaras turbulence model with **DNW-NWB Wind Tunnel**

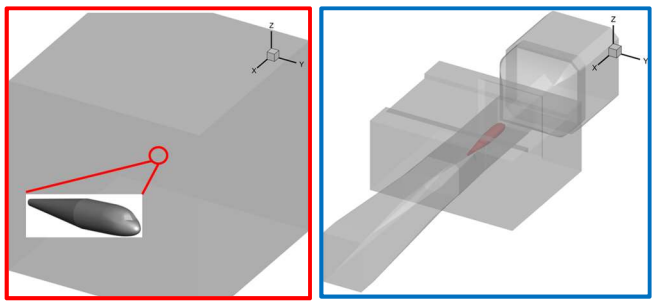

Figure 3: CFD simulation setup with farfield (left) and wind tunnel zones (right)

Fig. 3 shows the cockpit model along with cylindrical fuselage once inside the farfield zone and once inside an entire wind tunnel which includes individual zones for nozzle, diffusor, test-section, breather etc. Different turbulence models were implemented in order to check the effect of turbulence on the pressure gradients.

Results

Because of the cockpit shape, the velocity at 0.33m in x-direction – Fig. 4 (left), becomes minimum. Fig. 4 (right) represents velocity profile, normalized by local free-stream velocity, on this minimum velocity point. A flow separation i.e. negative local velocity near wall is observed.

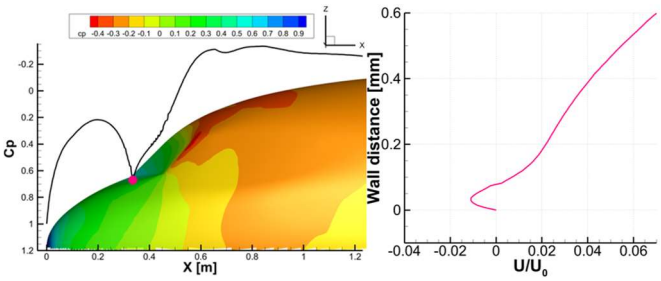

Figure 4: Cp curve in x-direction indicating minimum velocity point (left) and BL velocity profile at that point (right)

The inverted parabolic cp curve (until X= 0.33m) indicates the increase and then sudden decrease in local velocity till it reaches its relative minimum. However, the flow slowly accelerates again over the windshield reaching its maximum at the top of the cockpit.

To understand more in detail, total pressure BL profiles for the measured positions are further discussed. These total pressure profiles are normalized by the free-stream total pressure $p_{t\infty}$ and are plotted against wall normal distance.

On Windshield - Position 1

For this position, the rake was installed over the cockpit windshield. The velocity effect on pressure gradient was tested by keeping angle of attack constant ($\alpha = 3°$) and simultaneously changing the free stream velocity from 30-60m/s. As seen in Fig. 5 (left), the BL pressure gradient increases with the increase in U_∞. This change can also be projected for boundary layer thickness (δ) i.e. δ increases with the increase in U_∞.

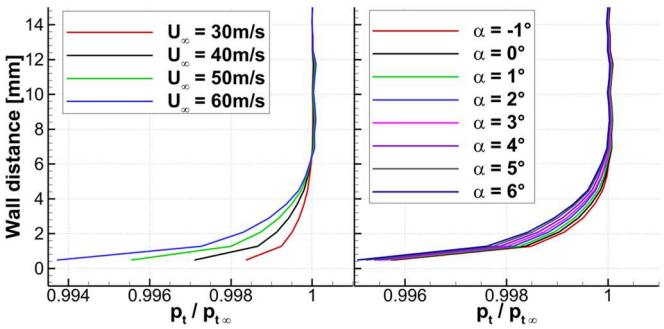

Figure 5: BL profile velocity variation (left) and angle of attack variation (right) for position 1

Similarly, the angle of attack effect was determined by varying it from -1° to 6°and letting U_∞ constant at 50m/s. The pressure gradient changes with the change in α (Fig. 5 right), but interestingly there are no irregularities in the BL profiles noticed with this variation.

On Top - Position 7 and 10 (Streamwise direction)

Looking from position 7 to 10, δ increases by approximately 2.3mm. Fig. 6 shows the comparison of experimental results with the CFD simulations once with Farfield (black line) and with entire wind tunnel (green line).

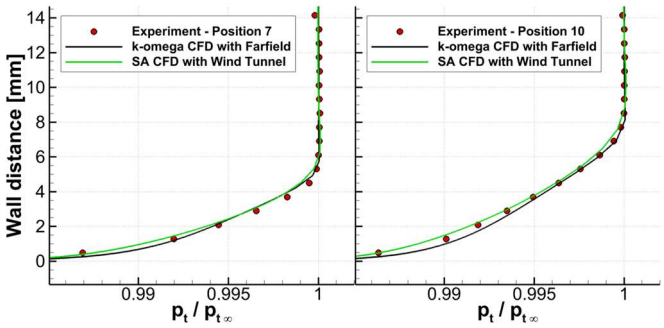

Figure 6: Comparison of BL profiles with simulations for position 7 (left) and position 10 (right)

BL profiles for both the positions are in good alignment with the simulations. In the streamwise direction, position 10 has lower pressure gradient compared to the position 7, hence lower wall shear stress (τ_ω) and lower friction velocity (u_τ). This implies that the boundary layer for position 10 develops slowly which in return gives higher δ. Another important boundary layer flow parameter is the boundary layer displacement thickness (δ^*), which also increases from 7 to 10, implying that there is more boundary layer effect at this point in the streamwise direction.

On Side - Position 19 and 21 (Streamwise direction)

Position 19 is located on the side of the cockpit, behind the windshield. Fig. 7 shows plots similar to position 1, to study the velocity along with the angle of attack effect. At a glance, a bump in the boundary layer profile is noticed for higher velocities (40-60m/s) and for angles of attack from 2°-4°. The BL profile for lower angles (α = -1°,0° and 1°) is consistent i.e. no bump exists.

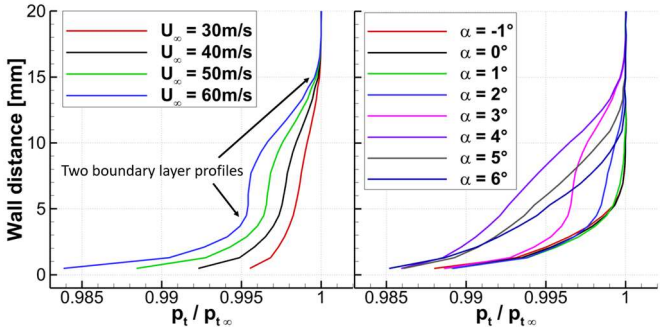

Figure 7: BL profile velocity variation (left) and angle of attack variation (right) for position 19

From the contour plot (Fig. 8), it can be clearly determined that the positions on the side region of the cockpit is not only affected by the flow coming from the nose, which has larger characteristic length, but also affected by another flow coming from the windshield, having smaller characteristic length. This effect makes the flow along the cockpit side more complex and its significance can be clearly visible in the measured wall pressure spectra [4].

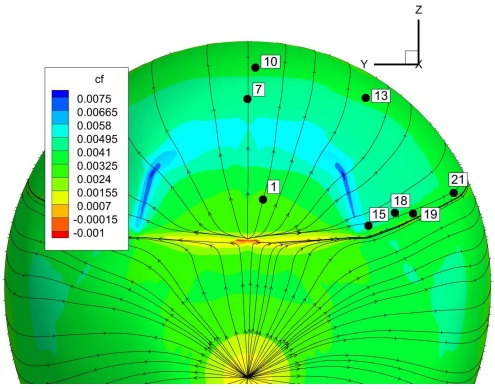

Figure 8: Friction coefficient contour plot

Upon assessment, the boundary layer bump disappears from position 19 to 21, giving only one BL profile. There could be mainly two theories (discussed in the following section) explaining this circumstance. Additionally, the numerical simulations using standard turbulence model deviate from the experimental data, see Fig. 9. These models on one hand are robust and accurate for fairly simple flow structures, as seen for positions 7 and 10, but for such a peculiar flow conditions a turbulence model such as RSM model is required which can resolve flow anisotropy and can directly compute individual Reynolds stress components.

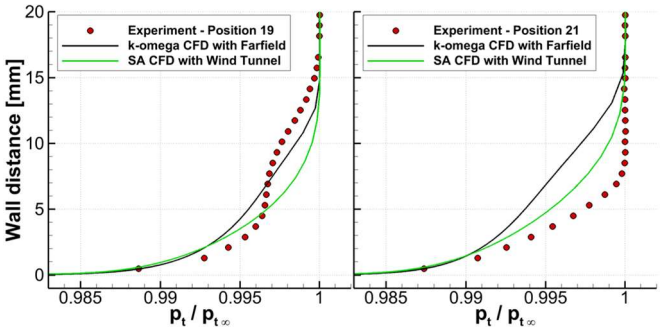

Figure 9: Comparison of BL profiles with simulations for position 19 (left) and position 21 (right)

Assumption/ Theory: 1

Two boundary layer profile

Behind the windshield, there could be the overlapping of two flows and the interaction of turbulent eddies within the boundary layer that creates two boundary layer profiles – Fig. 7. Resulting into, thinner BL thickness (~4.5mm) due to flow from the windshield and thicker δ (~16mm) due to flow from the nose. Eventually in the streamwise direction – Fig. 9, δ due to flow from the windshield increases by ~2.5mm (from 4.5mm to 7mm) and a part of the flow coming from the nose mixes with another flow and other part simultaneously dissipates into the free stream; finally left with one BL profile.

Assumption/ Theory: 2

Flow separation bubble at windshield

With the help of RSM turbulence method unsteady flow features were resolved for all three components, as e.g. shown in Fig. 10. Hao and Wang [6] showed velocity profiles for flow separation, reattachment and recovery and related recirculation bubble with negative skin-friction coefficient. In Fig. 10, the negative skin-friction coefficient is visible at the bottom of the windshield. So, the recirculation bubble of marginal size can be seen.

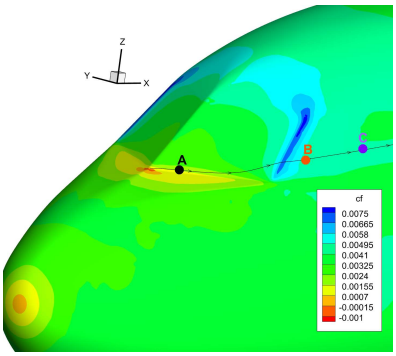

Figure 10: Contour plot of friction coefficient

Point A (black) is located near to the recirculation bubble, point B (orange) and point C (purple) are in the streamwise direction. Fig. 11 shows BL velocity and turbulent kinetic energy profiles of these three points. Both parameters are normalized by local free-stream velocity U_0. This local free-stream velocity increases from point A – C.

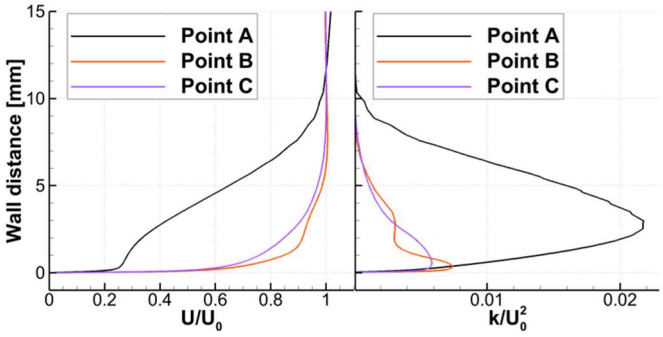

Figure 11: Comparison of velocity profiles (left) and turbulent kinetic energy profiles (right) for point A, B and C

The velocity profiles for point A and B seems to be alike to the velocity profiles described by Hao and Wang [6] in recovery region, where the flow reattaches after its separation. Point C and position 21 exhibit similar behaviour – i.e. a smooth profile without any notice of a bump.

Le et al. [7] also compared his turbulent flow simulation with Jovic & Driver experiment and represented Reynolds stress profiles for the recovery region. Thus, turbulent kinetic energy (TKE) profiles for points A, B and C are shown in Fig. – 11 (right). After the reattachment, point A has higher TKE and moving further in the streamwise direction, TKE decreases as seen in point B. Besides, point B has a near wall peak with irregular TKE profile which is not noticed for any other points, suggesting relatively high wall shear stress.

Conclusion

In the current framework, a thorough flow analysis was performed on a large-scale cockpit model. A turbulent flow was observed right on the model nose position and consequently higher boundary layer pressure gradients were obtained at all the measured cockpit positions.

The cockpit shape causes local flow separation and moreover complex flow turbulence on the side. This complex flow structure results into a bump in the boundary layer profiles, which is clearly noticed in the experimental data but cannot be computed using one- and two- equation turbulence models. A detailed turbulence model, here RSM model, has been adopted to capture critical turbulent flow condition. Although, this turbulence model reproduced similar results to that of the experiment, the reason for this bump is yet to be investigated.

Furthermore, the necessary boundary layer parameters for the formulation of empirical model can be extracted from the CFD simulations, as the aerodynamical study showed here an overall good agreement between the experiments and the simulations.

Acknowledgement

This research work was conducted under the project INTeriOr Noise and VibrATion Evaluation. A huge thanks to all the co-authors and the colleagues at DLR Braunschweig, who helped with their insight and knowledge.

Literature

[1] Goody M. C., “Empirical Spectral Model of Surface Pressure Fluctuations”, AIAA Journal Vol. 42, No. 9, 2004, pp. 1788-1794. DOI: 10.2514/1.9433

[2] Rozenberg Y., Robert G. and Moreau S., “Wall-Pressure Spectral Model Including the Adverse Pressure Gradient Effects”, AIAA Journal Vol. 50, No. 10, 2012, pp. 2168-2179. DOI: 10.2514/1.J051500

[3] Hu N. and Herr M., “Characteristics of Wall Pressure Fluctuations for a Flat Plate Turbulent Boundary Layer with Pressure Gradients”, 22nd AIAA/CEAS Aeroacoustics Conference, 2016. DOI: 10.2514/6.2016-2749

[4] Jansen M., Naik H., Rossignol K. and Nan H., “Experimental Investigations on a Large-Scale Cockpit-Fuselage Model for Surface Pressure Fluctuations”, DAS|DAGA, 2025

[5] Salze E., Prigent S., Jondeau E. and Bailly C., “Experimental Investigation of Wall-Pressure Fluctuations on a Full-Scale Business Jet”, e-Forum Acusticum, 2020, pp. 727-730. DOI: 10.48465/fa.2020.0255, hal-03229449

[6] Hao J. and Wang M., “Flow Noise from Swept Steps in Turbulent Boundary Layers”, 19th AIAA/CEAS Aeroacoustics Conference, 2013. DOI: 10.2514/6.2013-2248

[7] Le H., Moin P. and Kim J., “Direct numerical simulation of turbulent flow over a backward-facing step”, Journal of Fluid Mechanics Vol. 330, pp. 349-374, 1997. DOI: 10.1017/S0022112096003941